Supplement of Atmos. Chem. Phys., 26, 1339–1357, 2026
https://doi.org/10.5194/acp-26-1339-2026-supplement

Atmospheric Chemistry and Physics
Open Access
EGU

Supplement of

Air quality impacts of stratospheric aerosol injections are likely small and mainly driven by changes in climate, not aerosol settling

Cindy Wang et al.

Correspondence to: Cindy Wang (cindywang@cornell.edu)

A comparison of the attributable fraction (AF) used in this study to calculate $PM_{2.5}$ and ozone associated mortality is presented in Fig. S1. The AF for $PM_{2.5}$ (NCD+LRI) is lower per $\mu g\,m^{-3}$ of $PM_{2.5}$ because its harm is spread across many diseases, while ozone's AF is higher per ppb for cardiovascular and respiratory diseases because it acts more acutely and specifically on those systems. In Fig. S1a, $PM_{2.5}$ exhibits a near-linear dose–response relationship with mortality, indicating that risks accumulate gradually. In contrast, Fig. S1b shows that ozone has a steeper curve at lower doses, meaning even small increases in surface O_3 can disproportionately elevate the risk of cardiovascular and respiratory diseases (Burnett and Cohen, 2020).

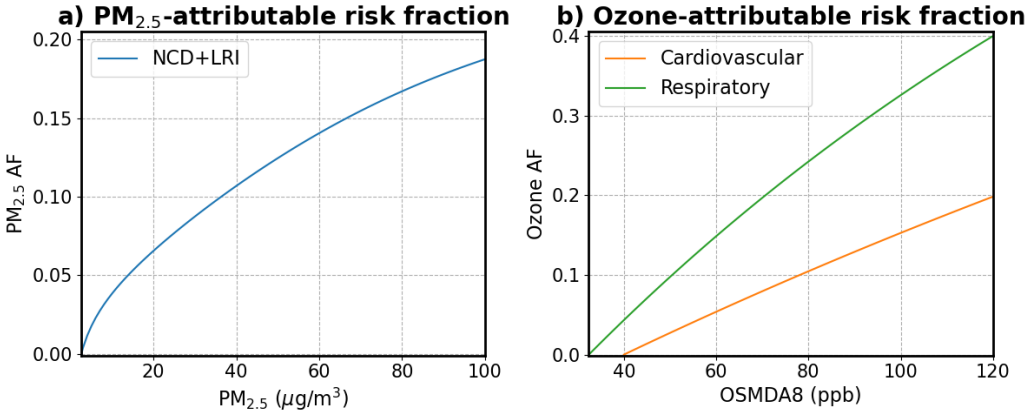

Figure S1: (a) Attributable fraction of mortality due to $PM_{2.5}$ exposure as a function of $PM_{2.5}$ concentration, based on the mean relative risk across age groups for non-communicable diseases (NCD) and lower respiratory infections (LRI). (b) Attributable fraction of mortality due to ozone (OSMDA8) exposure, with separate curves for cardiovascular and respiratory causes. Risk functions are based on excess mortality relative to baseline thresholds (2.5 ppm for NCD+LRI, 40 ppb for cardiovascular and 32.4 ppb for respiratory outcomes).

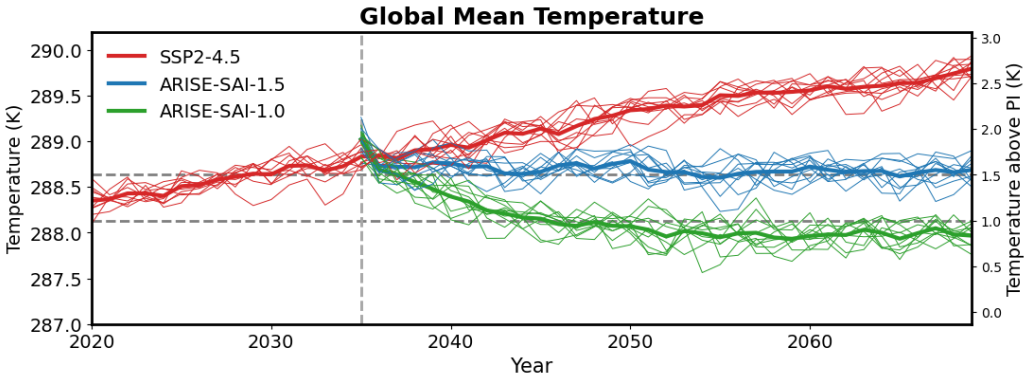

Figure S2: Global mean surface temperature for SSP2-4.5, ARISE-SAI-1.5, and ARISE-SAI-1.0 simulations. Thin lines represent individual ensemble members and thick lines represent the ensemble mean.

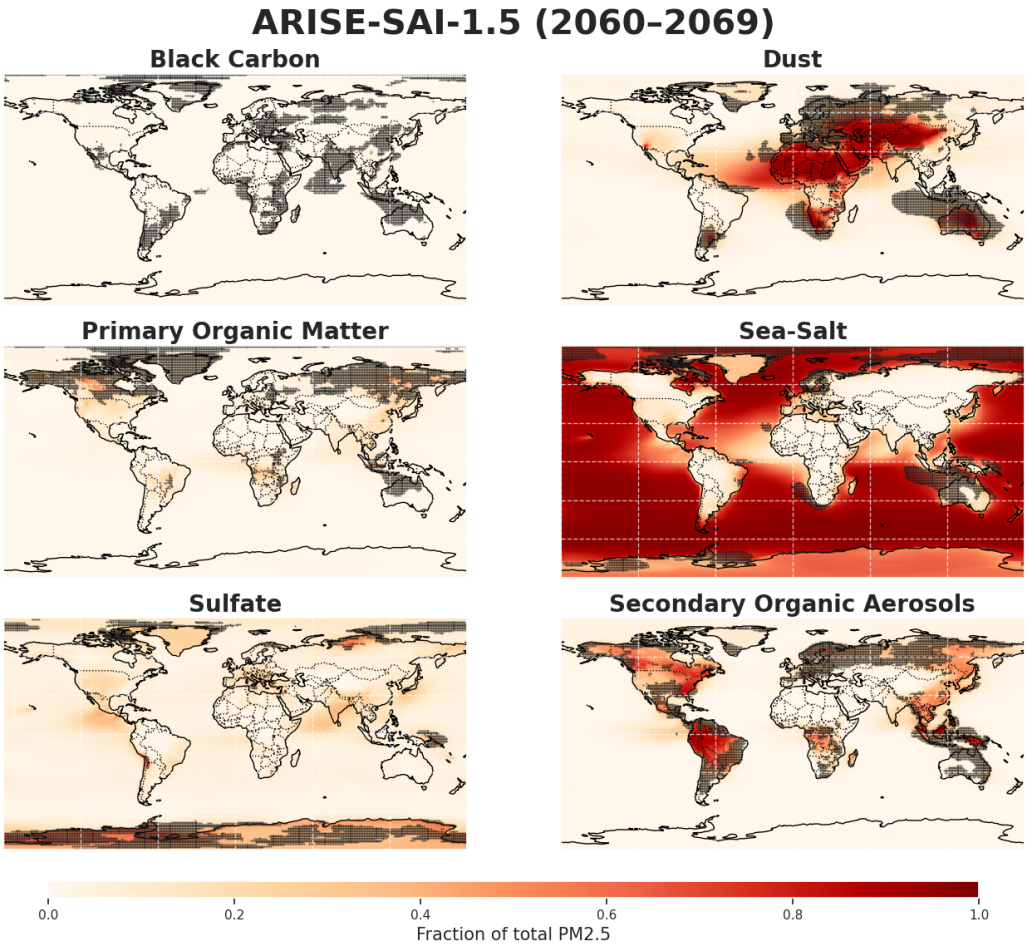

Figure S3: Mean fractional contribution of $PM_{2.5}$ species under ARISE-SAI-1.5 (2060–2069). Color shading shows the ensemble-mean fraction of each species relative to total $PM_{2.5}$. Stippling marks regions where the ensemble standard deviation exceeds the 95th percentile, indicating high internal variability.

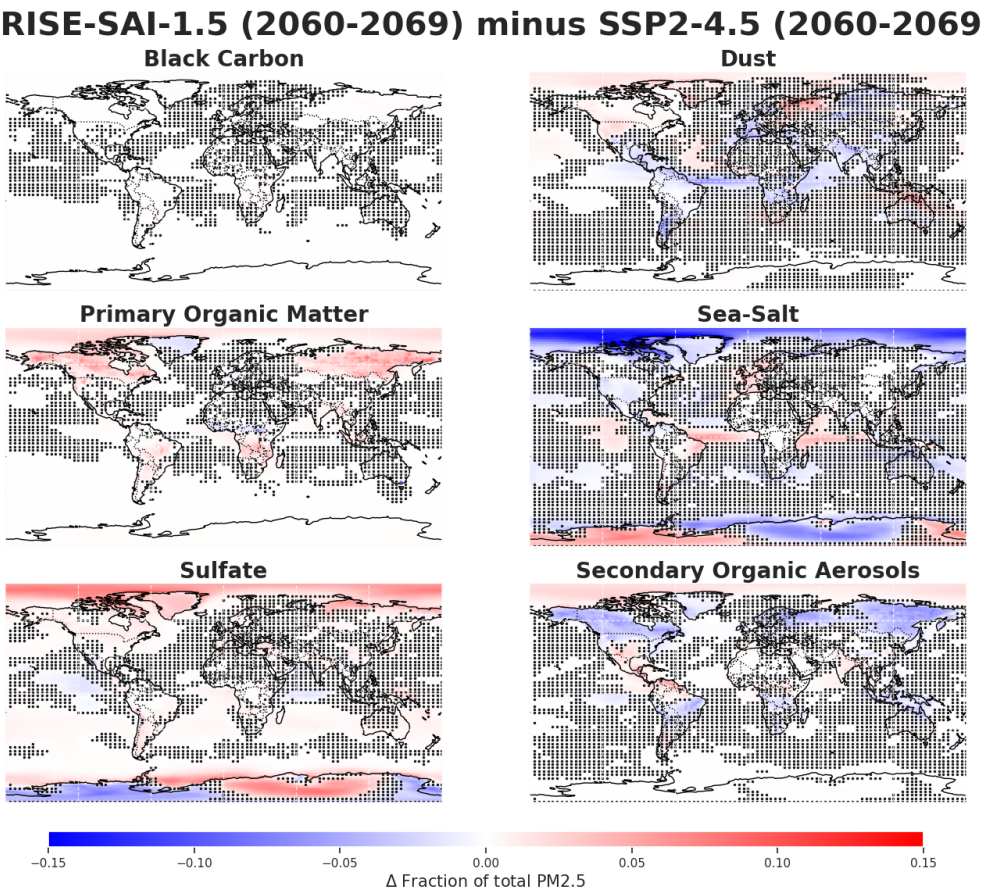

Figure S4: Changes in the fractional contribution of $PM_{2.5}$ species between ARISE-SAI-1.5 and SSP2-4.5 (2060–2069). Positive (red) values indicate an increased contribution under ARISE-SAI-1.5, while negative (blue) values indicate a decreased contribution. Sparse stippling marks areas where changes are not statistically significant ($p>0.05$) based on a two-sided t-test across ensemble members.

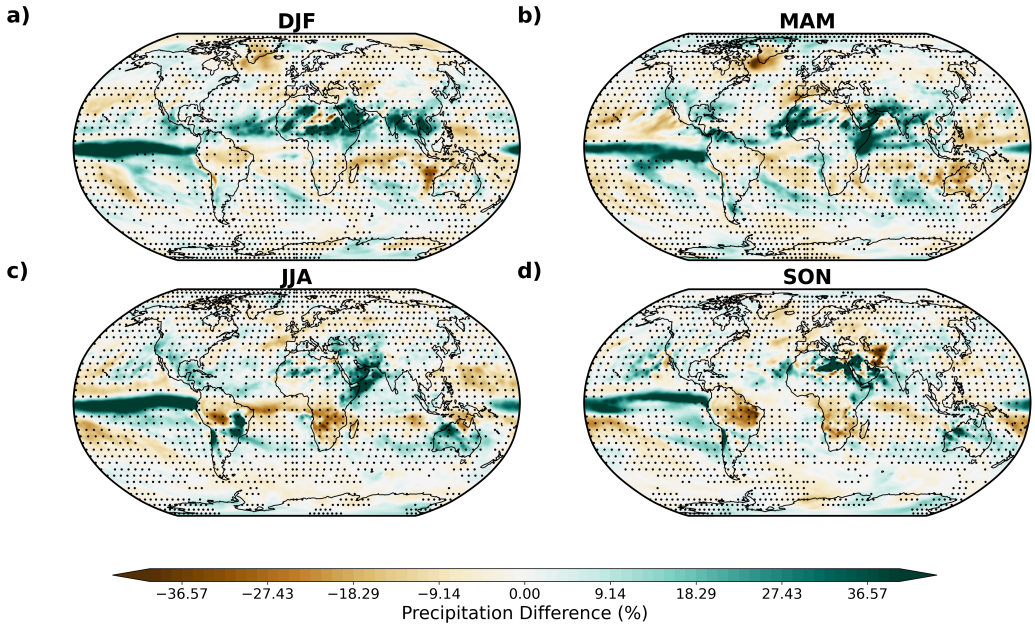

Figure S5: Seasonal (DJM, MAM, JJA and SON) zonal-mean % differences in precipitation for ARISE-SAI-1.5 (2060–2069) minus SSP2-4.5 (2030–2039). The stippling indicates areas where differences between ARISE-SAI-1.5 and SSP2-4.5 are not statistically significant ($p>0.05$) based on a t-test performed across all 10 ensemble members.

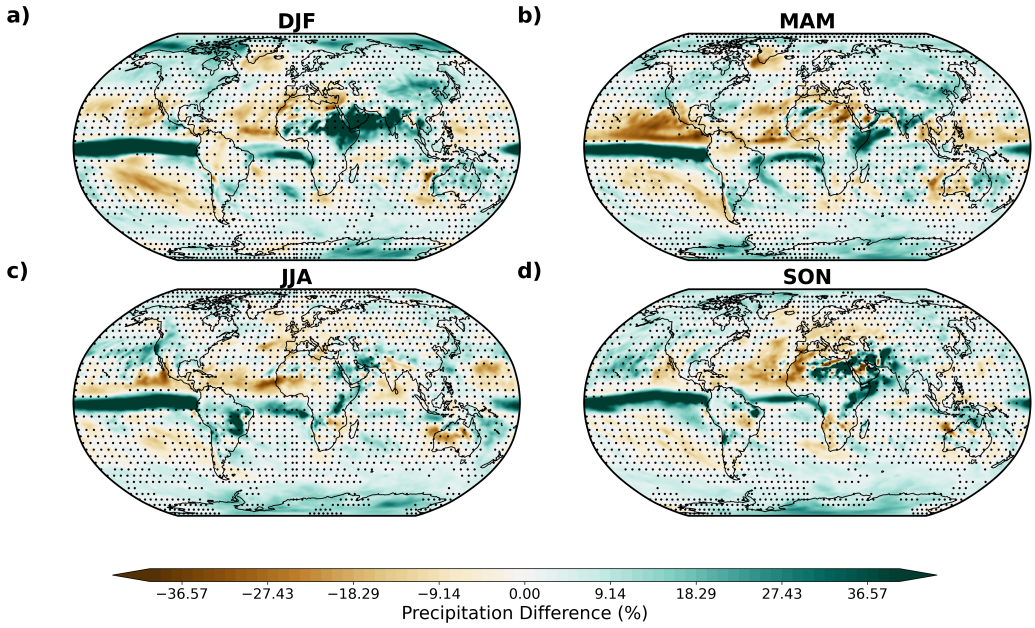

Figure S6: Seasonal (DJM, MAM, JJA and SON) zonal-mean % differences in precipitation for SSP2-4.5 (2060–2069) minus SSP2-4.5 (2030–2039). The stippling indicates areas where differences between ARISE-SAI-1.5 and SSP2-4.5 are not statistically significant ($p>0.05$) based on a t-test performed across all 10 ensemble members.

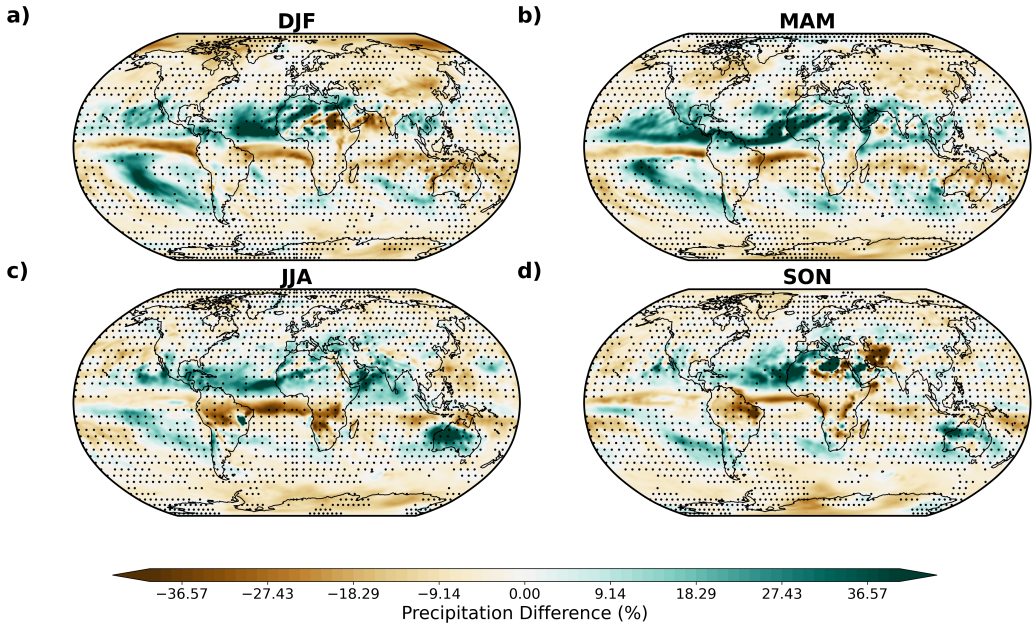

Figure S7: Seasonal (DJM, MAM, JJA and SON) zonal-mean % differences in precipitation for ARISE-SAI-1.5 (2060–2069) minus SSP2-4.5 (2060–2069). The stippling indicates areas where differences between ARISE-SAI-1.5 and SSP2-4.5 are not statistically significant ($p>0.05$) based on a t-test performed across all 10 ensemble members.

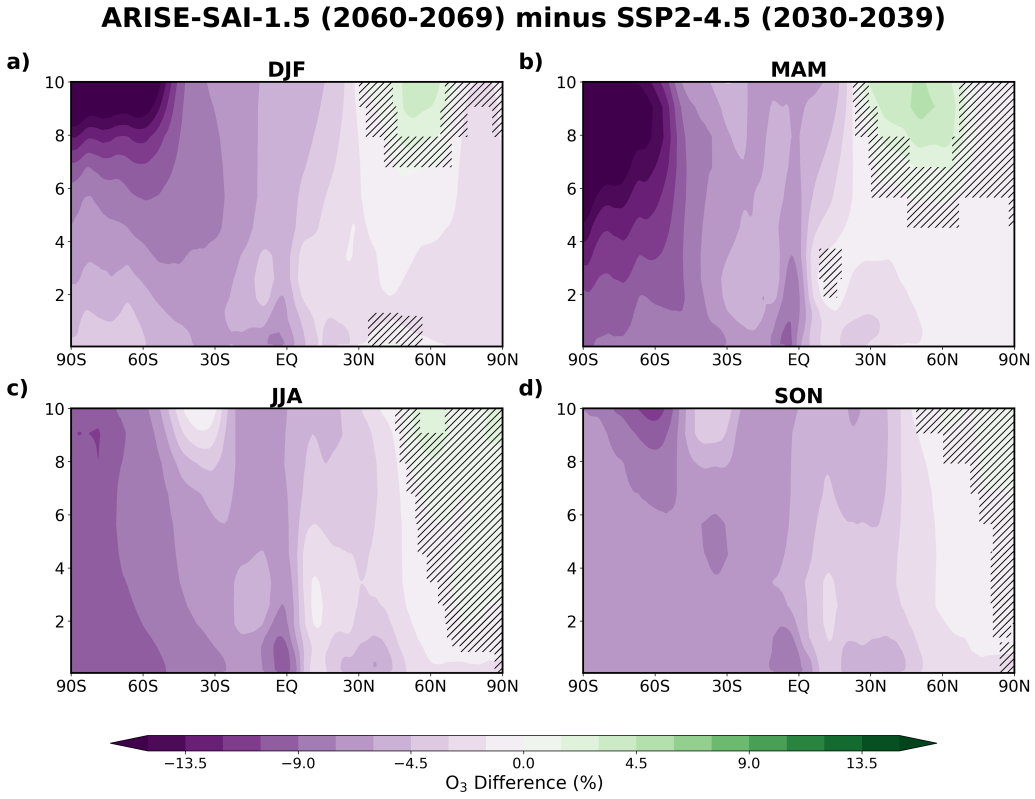

Figure S8: Seasonal (DJM, MAM, JJA and SON) zonal-mean % differences in O_3 for ARISE-SAI-1.5 (2060–2069) minus SSP2-4.5 (2030–2039). The stippling indicates areas where differences between ARISE-SAI-1.5 and SSP2-4.5 are not statistically significant ($p>0.05$) based on a t-test performed across all 10 ensemble members.

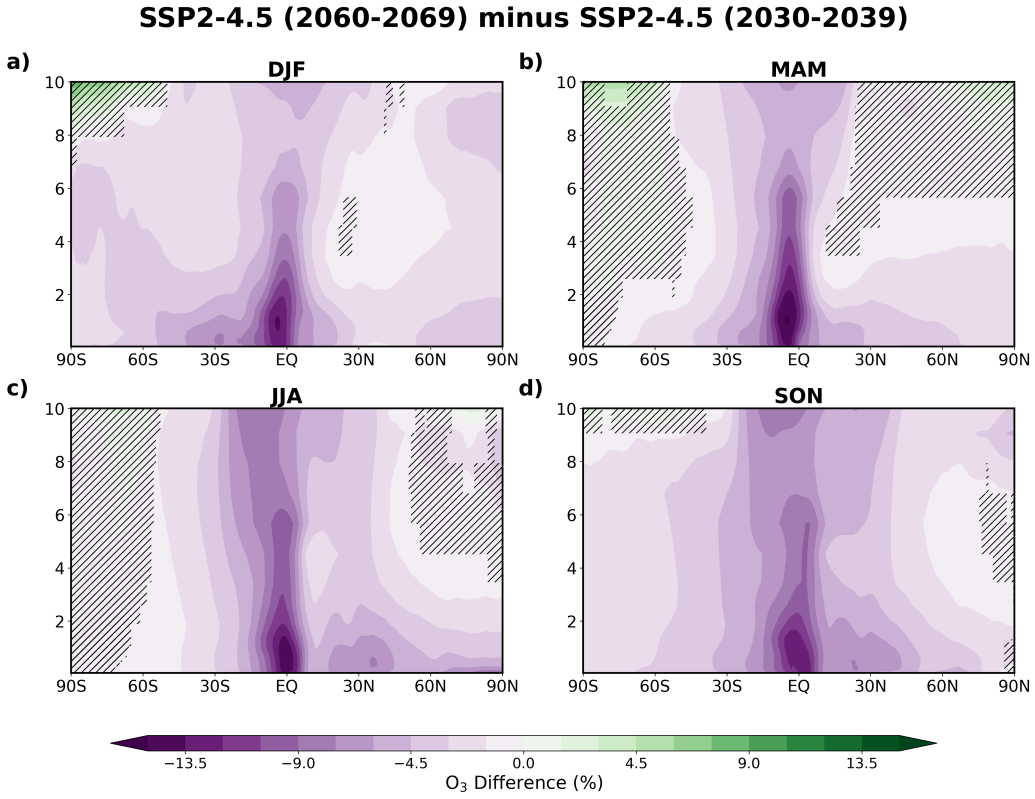

Figure S9: Seasonal (DJM, MAM, JJA and SON) zonal-mean % differences in O_3 for SSP2-4.5 (2060–2069) minus SSP2-4.5 (2030–2039). The stippling indicates areas where differences between ARISE-SAI-1.5 and SSP2-4.5 are not statistically significant ($p>0.05$) based on a t-test performed across all 10 ensemble members.

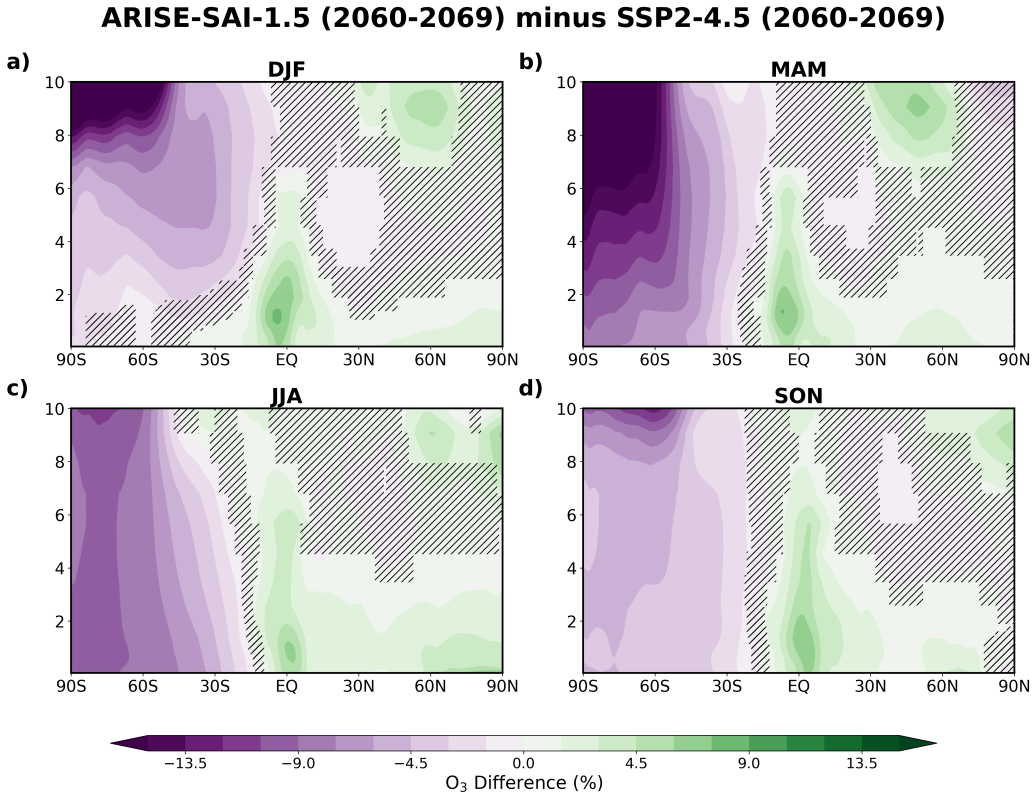

Figure S10: Seasonal (DJM, MAM, JJA and SON) zonal-mean % differences in O_3 for ARISE-SAI-1.5 (2060–2069) minus SSP2-4.5 (2060–2069). The stippling indicates areas where differences between ARISE-SAI-1.5 and SSP2-4.5 are not statistically significant ($p>0.05$) based on a t-test performed across all 10 ensemble members.

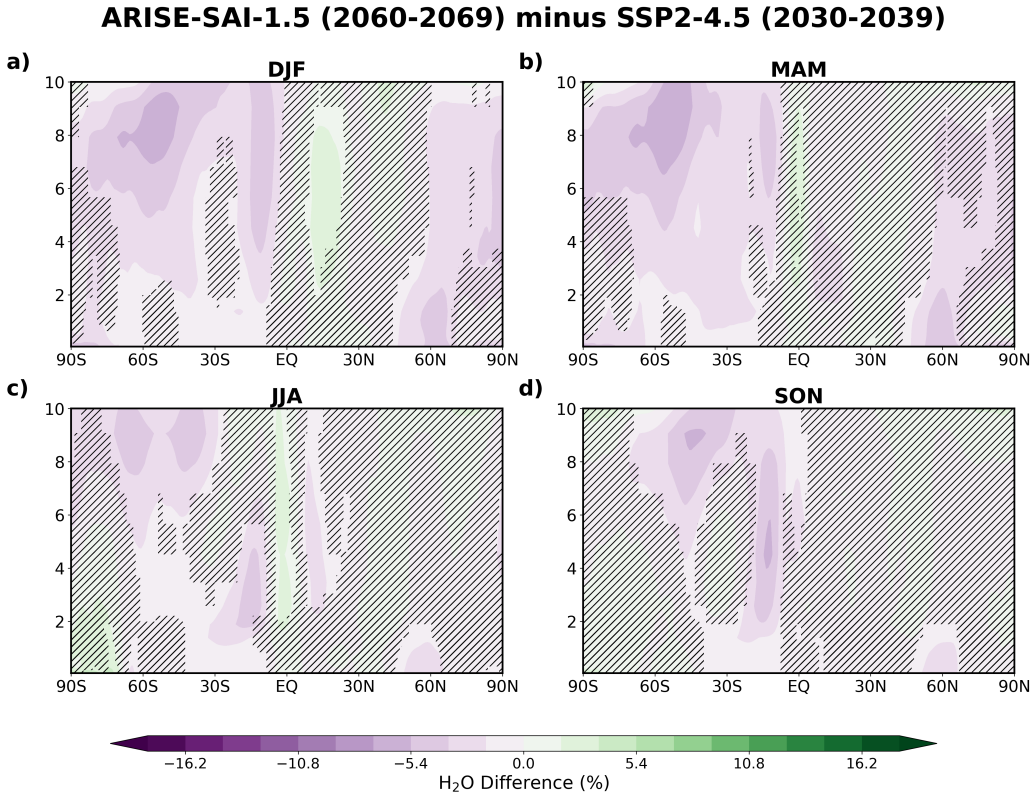

Figure S11: Seasonal (DJM, MAM, JJA and SON) zonal-mean % differences in water vapor concentration (H_2O) for ARISE-SAI-1.5 (2060–2069) minus SSP2-4.5 (2030–2039). The stippling indicates areas where differences between ARISE-SAI-1.5 and SSP2-4.5 are not statistically significant ($p>0.05$) based on a t-test performed across all 10 ensemble members.

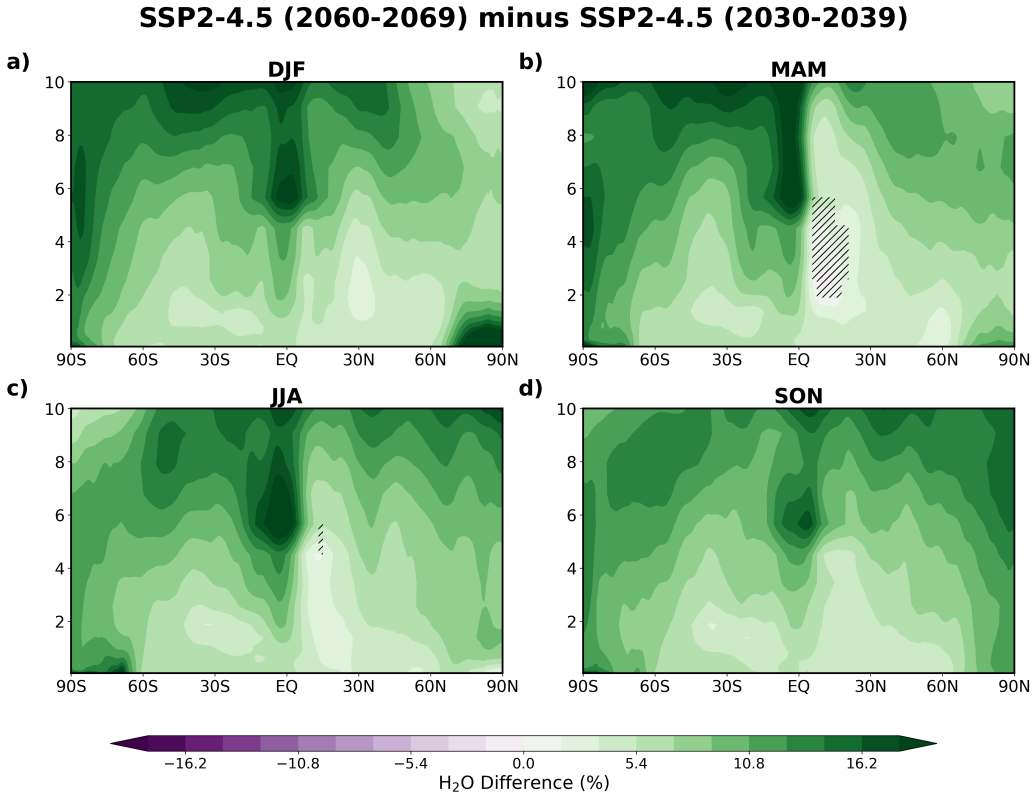

Figure S12: Seasonal (DJM, MAM, JJA and SON) zonal-mean % differences in water vapor concentration (H_2O) for SSP2-4.5 (2060–2069) minus SSP2-4.5 (2030–2039). The stippling indicates areas where differences between ARISE-SAI-1.5 and SSP2-4.5 are not statistically significant ($p>0.05$) based on a t-test performed across all 10 ensemble members.

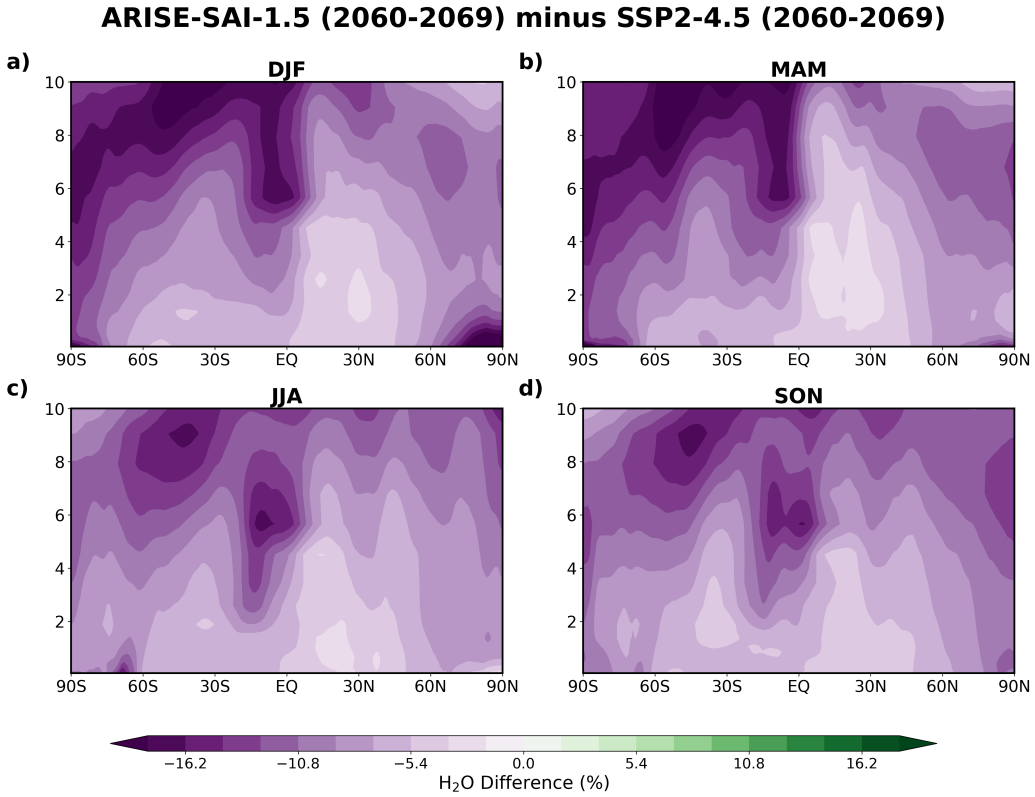

Figure S13: Seasonal (DJM, MAM, JJA and SON) zonal-mean % differences in water vapor concentration (H_2O) for ARISE-SAI-1.5 (2060–2069) minus SSP2-4.5 (2060–2069). The stippling indicates areas where differences between ARISE-SAI-1.5 and SSP2-4.5 are not statistically significant ($p>0.05$) based on a t-test performed across all 10 ensemble members.

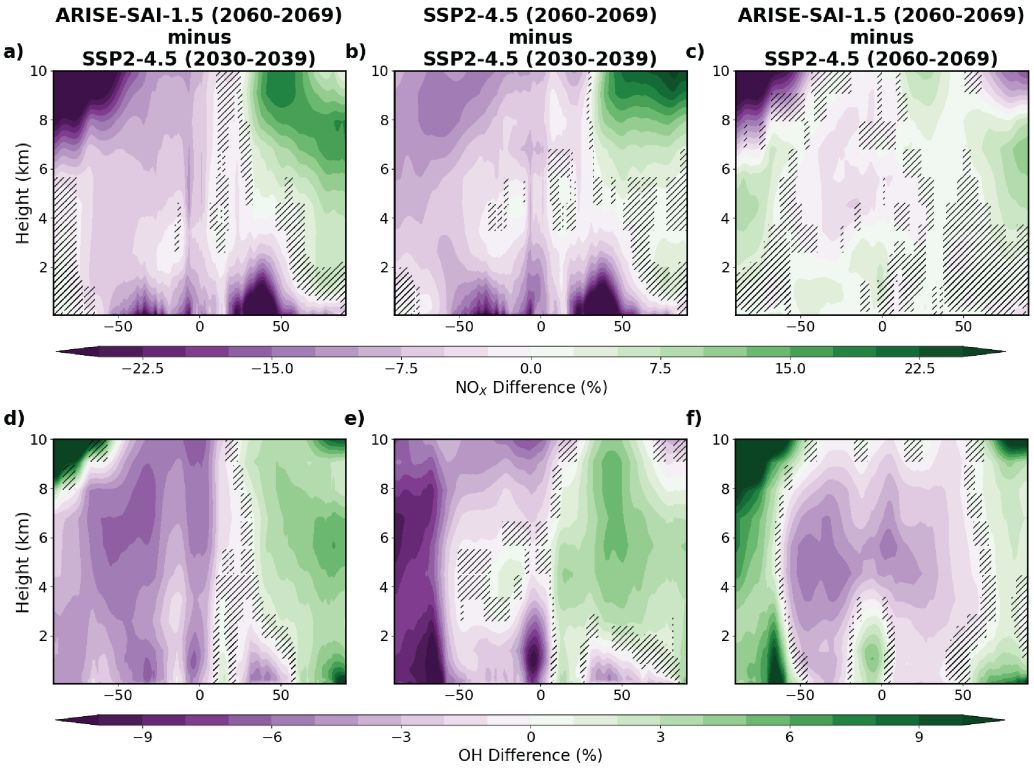

Figure S14: Zonal-mean % differences in NO_X (a-b), and OH (d-f) concentrations are presented for ARISE-SAI-1.5 (2060–2069) minus SSP2-4.5 (2030–2039), SSP2-4.5 (2060–2069) minus SSP2-4.5 (2030–2039), and ARISE-SAI-1.5 (2060–2069) minus SSP2-4.5 (2060–2069). The stippling indicates areas where differences between ARISE-SAI-1.5 and SSP2-4.5 are not statistically significant ($p>0.05$) based on a t-test performed across all 10 ensemble members.

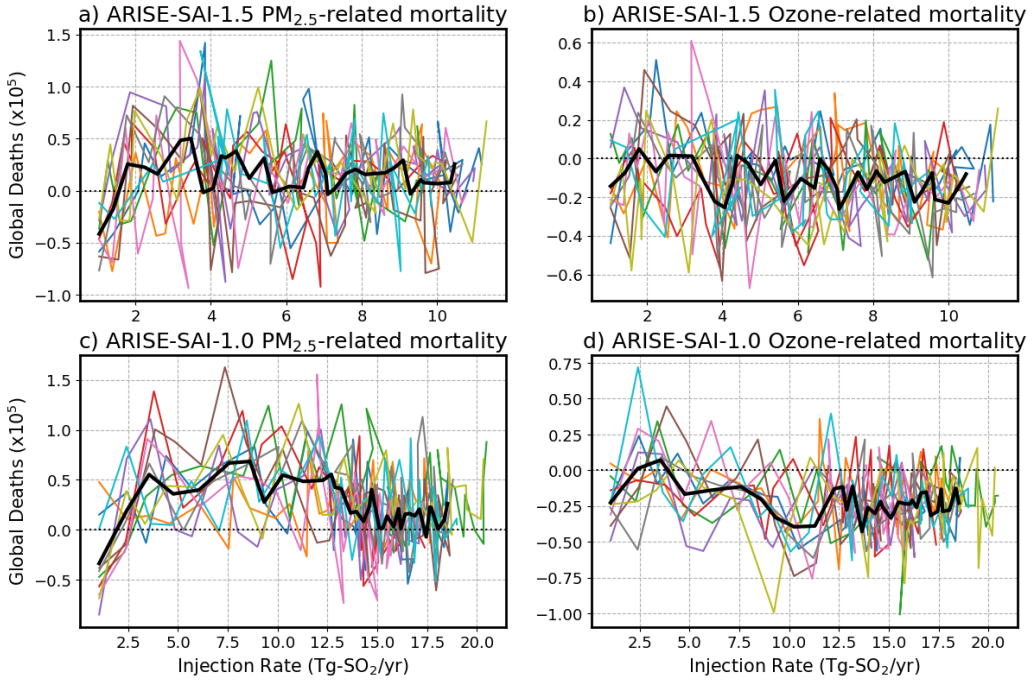

Figure S15: Global differences in air-pollution mortality between ARISE-SAI and SSP2-4.5 as a function of the total SO_2 injection rate for the first 35 simulation years. Panels show (a) $PM_{2.5}$-attributable mortality for ARISE-SAI-1.5, (b) ozone-attributable mortality for ARISE-SAI-1.5, (c) $PM_{2.5}$ for ARISE-SAI-1.0, and (d) ozone for ARISE-SAI-1.0. Colored lines indicate individual ensemble members, while the thick black line represents the 10-member ensemble mean.

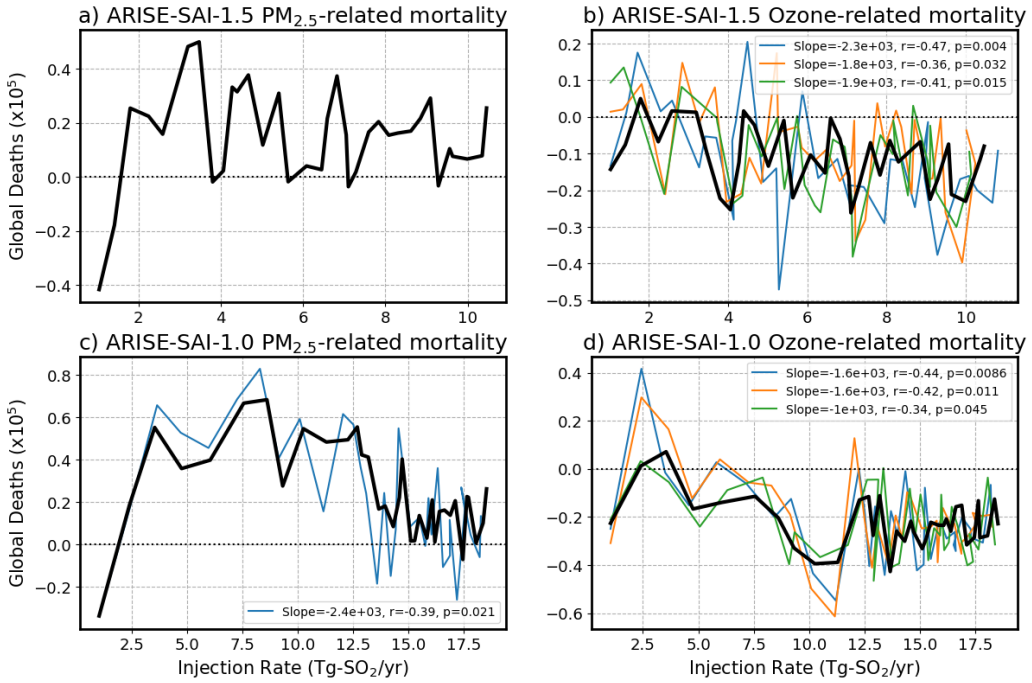

Figure S16: Global mortality differences between ARISE-SAI and SSP2-4.5 are shown as a function of the SO_2 injection rate over the first 35 years of simulation. Panels depict (a) $PM_{2.5}$-attributable mortality for ARISE-SAI-1.5, (b) ozone-attributable mortality for ARISE-SAI-1.5, (c) $PM_{2.5}$ for ARISE-SAI-1.0, and (d) ozone for ARISE-SAI-1.0. Colored lines represent ordinary least-squares fits from randomly selected 3-member ensemble subsets (10 draws), plotted only where significant linear relationships are detected ($p < 0.05$). Slopes, r-values, and p-values are annotated in the legend.

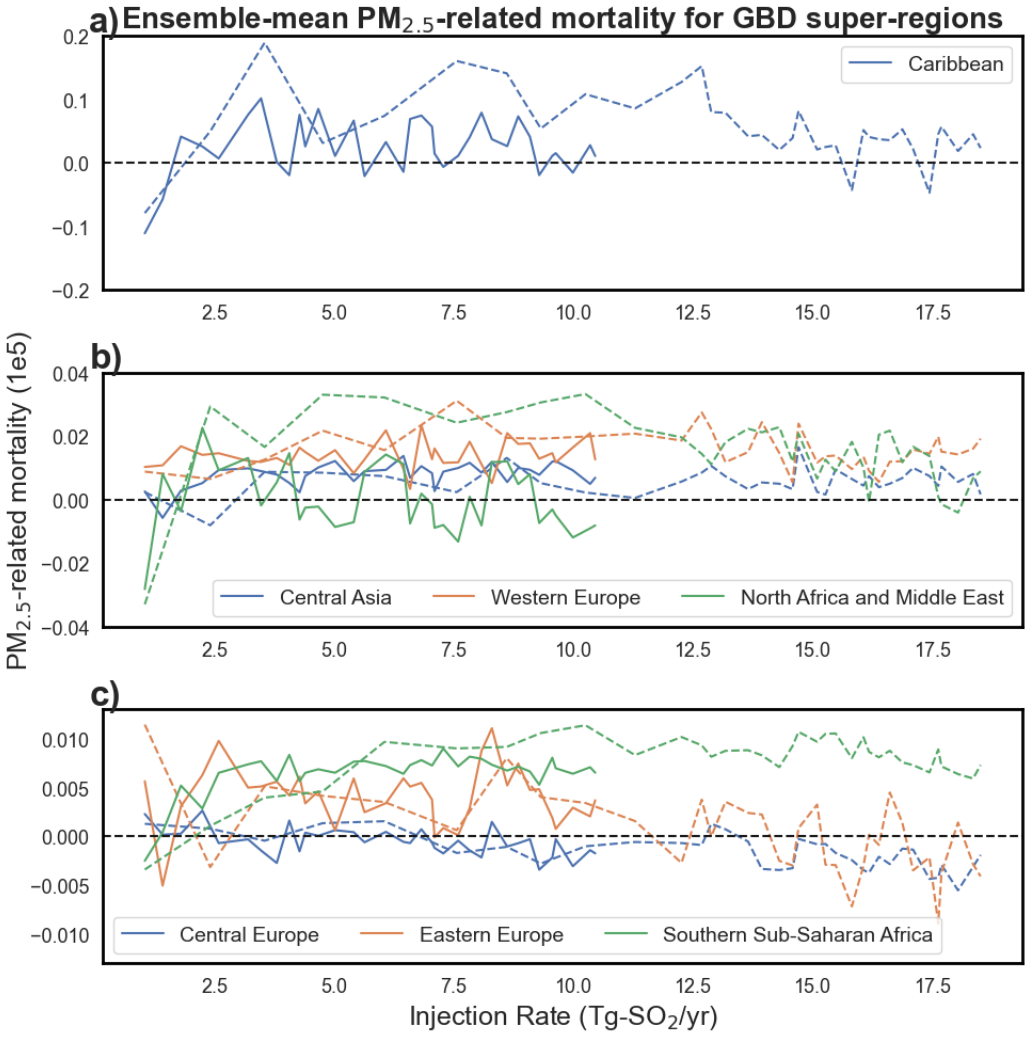

Figure S17: Ensemble-mean $PM_{2.5}$-related mortality differences (ARISE-SAI-1.5 minus SSP2-4.5) for selected GBD super-regions as a function of stratospheric SO_2 injection rate. The dashed line shows the corresponding PM2.5-related mortality differences for ARISE-SAI-1.0 minus SSP2-4.5.

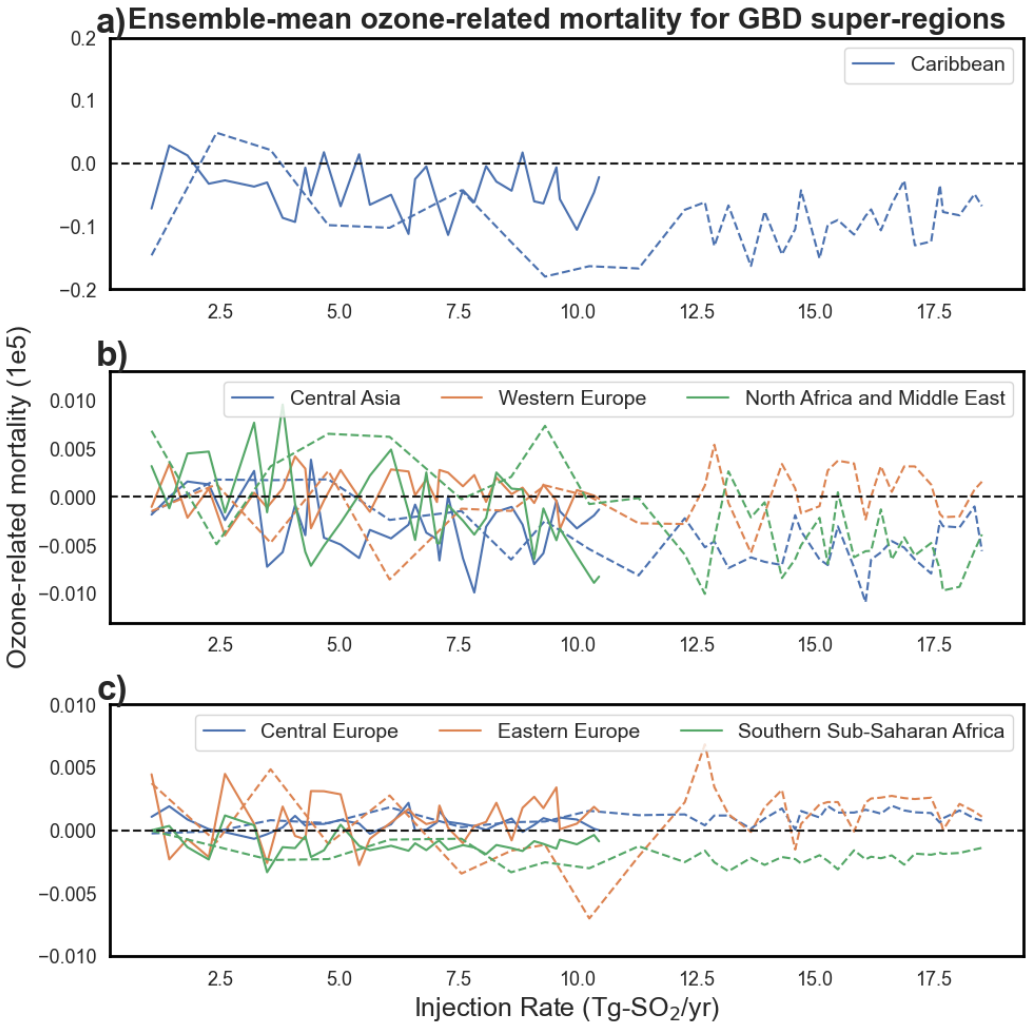

Figure S18: Ensemble-mean ozone-related mortality differences (ARISE-SAI-1.5 minus SSP2-4.5) for selected GBD super-regions as a function of stratospheric SO_2 injection rate. The dashed line shows the corresponding ozone-related mortality differences for ARISE-SAI-1.0 minus SSP2-4.5.

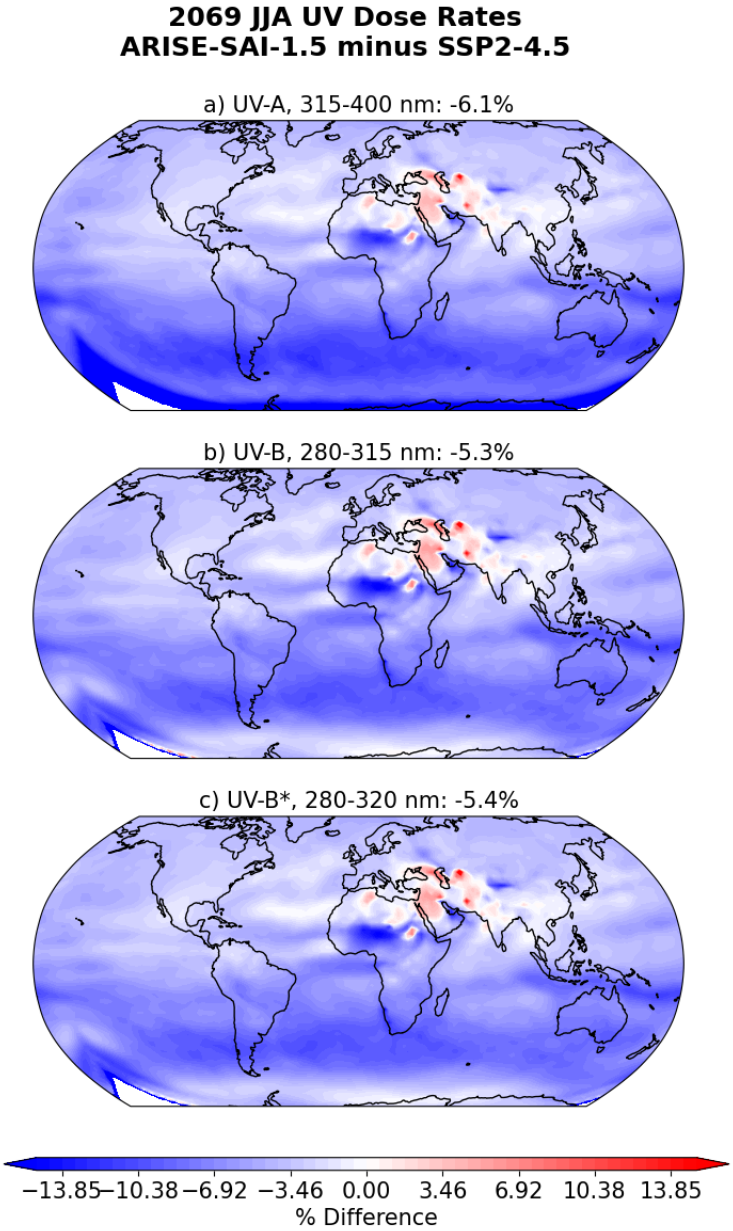

Figure S19: Percent differences in clear-sky midday UV dose rates for June-August (JJA) 2069 between ARISE-SAI-1.5 and SSP2-4.5 (one ensemble member), calculated with the Tropospheric Ultraviolet and Visible (TUV) model developed at NCAR (Madronich and Flocke, 1999): a) UV-A (315-400 NM), b) UV-B (280-315 nm), and c) UV-B* (280-320 NM). Global mean differences are shown in the figure titles.

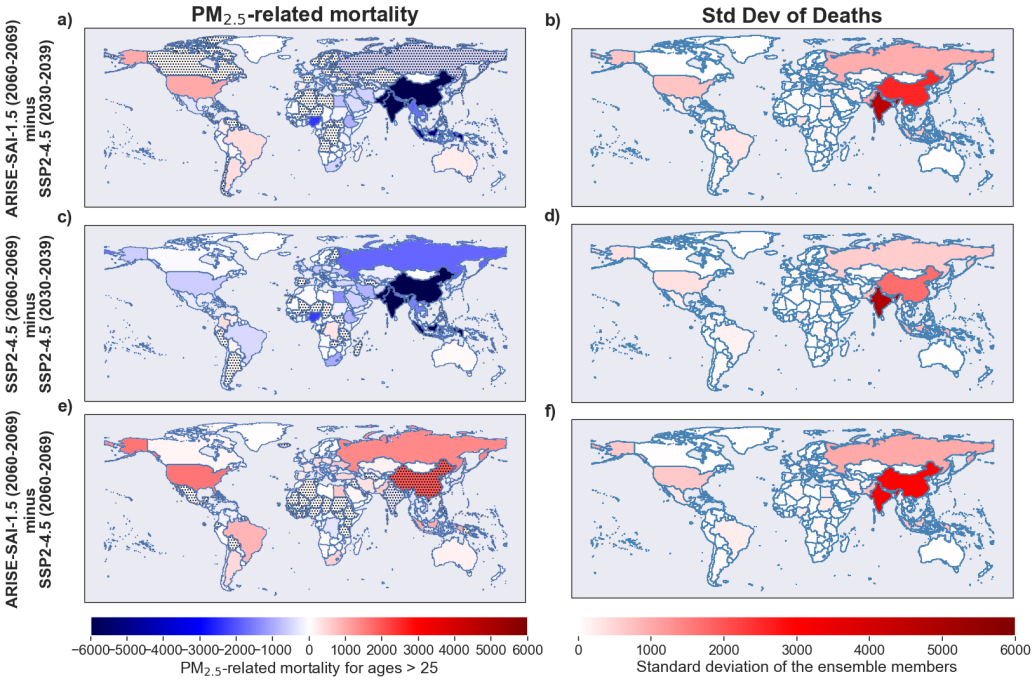

Figure S20: The ensemble-mean deaths from $PM_{2.5}$ for ages > 25. Stippling indicates countries where estimates of the $PM_{2.5}$-related mortality are not statistically significant across ensemble members at the 95% confidence level.

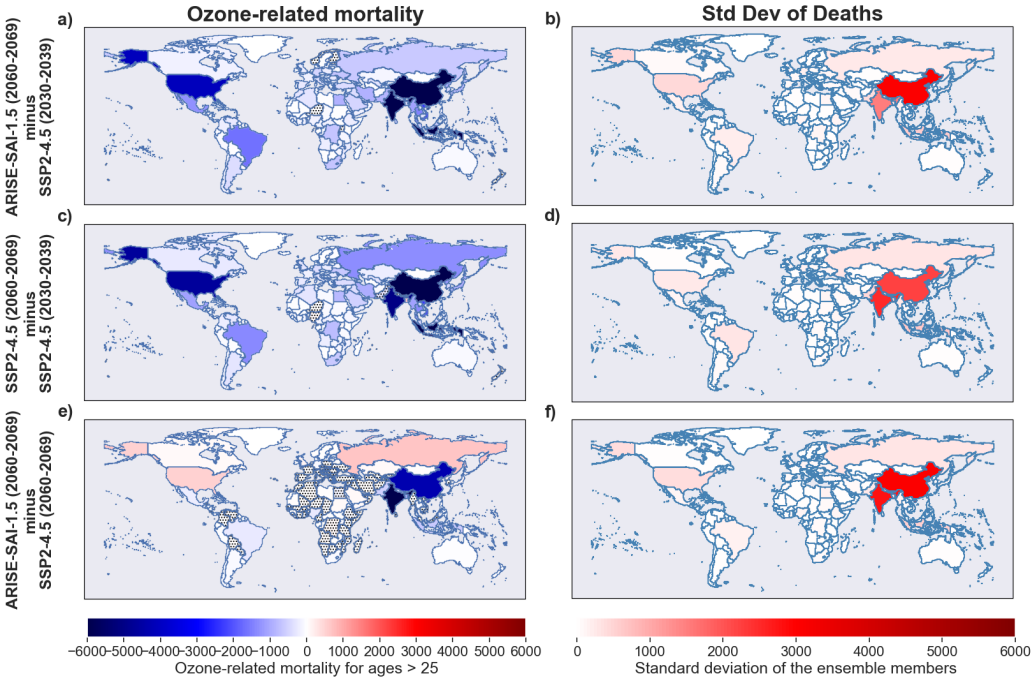

Figure S21: The ensemble-mean deaths from ozone for ages > 25. Stippling indicates countries where estimates of the ozone-related mortality are not statistically significant across ensemble members at the 95% confidence level.

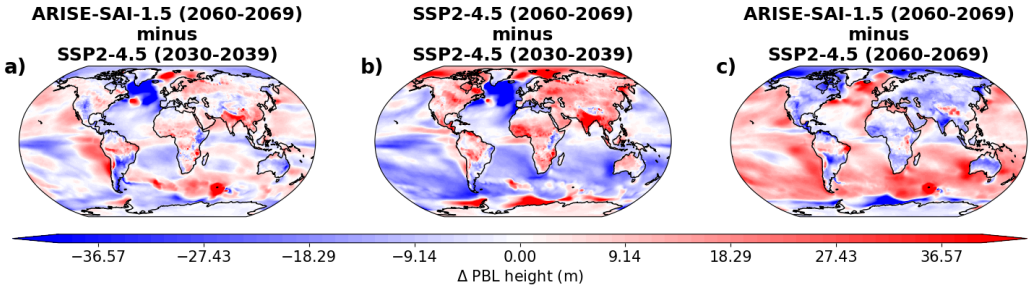

Figure S22: Planetary boundary layer height (PBLH) differences for ARISE-SAI-1.5 (2060–2069) minus SSP2-4.5 (2030–2039), SSP2-4.5 (2060–2069) minus SSP2-4.5 (2030–2039), and ARISE-SAI-1.5 (2060–2069) minus SSP2-4.5 (2060–2069).

References

Burnett, R. and Cohen, A.: Relative risk functions for estimating excess mortality attributable to outdoor PM2. 5 air pollution: Evolution and state-of-the-art, Atmosphere, 11, 589, 2020.

Madronich, S. and Flocke, S.: The Role of Solar Radiation in Atmospheric Chemistry, in: Environmental Photochemistry, edited by Boule, P., The Handbook of Environmental Chemistry, pp. 1–26, Springer, Berlin, Heidelberg, https://doi.org/10.1007/978-3-540-69044-3$_1$, 1999.